A Passivity Based Cartesian Impedance Controller for Flexible Joint Robots - Part II: Full State Feedback, Impedance Design and Experiments

Alin Albu-Schäffer, Christian Ott and Gerd Hirzinger
Institute of Robotics and Mechatronics, German Aerospace Center (DLR), Germany
Email: Alin.Albu-Schaeffer@dlr.de, Christian.Ott@dlr.de

***Abstract*— The paper presents a Cartesian impedance controller for ¤exible joint robots based on the feedback of the complete state of the system, namely the motor position, the joint torque and their derivatives. The approach is applied to a quite general robot model, in which also a damping element is considered in parallel to the joint stiffness. Since passivity and asymptotic stability of the controller hold also for varying damping matrices, some possibilities of designing those gain matrices (depending on the actual inertia matrix) are addressed. The passivity of the controller relies on the usage of only motor side measurements for the position feedback. A method is introduced, which provides the exact desired link side stiffness based on this motor position information. Experimental results are validating the proposed controller.**

I. Introduction

In the £rst part of this work [7], the design of a new passivity based Cartesian impedance controller was proposed for a ¤exible joint robot. The following model structure introduced by Spong [8] was used:

$$\boldsymbol{M}(\boldsymbol{q})\ddot{\boldsymbol{q}} + \boldsymbol{C}(\boldsymbol{q},\dot{\boldsymbol{q}})\dot{\boldsymbol{q}} + \boldsymbol{g}(\boldsymbol{q}) = \boldsymbol{\tau} + \boldsymbol{\tau}_{ext} \quad (1)$$

$$\boldsymbol{B}\ddot{\boldsymbol{\theta}} + \boldsymbol{\tau} = \boldsymbol{\tau}_m \quad (2)$$

$$\boldsymbol{\tau} = \boldsymbol{K}(\boldsymbol{\theta} - \boldsymbol{q}) \quad (3)$$

$\boldsymbol{q} \in \Re^n$ and $\boldsymbol{\theta} \in \Re^n$ are the link and motor side positions respectively. $\boldsymbol{M}(\boldsymbol{q}) \in \Re^{n\times n}$, $\boldsymbol{C}(\boldsymbol{q},\dot{\boldsymbol{q}})\dot{\boldsymbol{q}}$, $\boldsymbol{g}(\boldsymbol{q}) \in \Re^n$ are the components of the rigid body dynamics: inertia matrix, centripetal and Coriolis vector, and gravity vector. $\boldsymbol{\tau} \in \Re^n$ is the joint torque, $\boldsymbol{\tau}_{ext} \in \Re^n$ is the external torque acting on the robot and $\boldsymbol{\tau}_m \in \Re^n$ ist the motor torque. $\boldsymbol{K} = diag(K_i) \in \Re^{n\times n}$ and $\boldsymbol{B} = diag(B_i) \in \Re^{n\times n}$ are the diagonal, positive de£nite (p.d.) joint stiffness and joint inertia matrices, respectively.

The controller consists of a torque feedback loop which can be interpreted as a scaling of the motor inertia to a desired value $\boldsymbol{B}_\theta$:

$$\boldsymbol{\tau}_m = \boldsymbol{B}\boldsymbol{B}_\theta^{-1}\boldsymbol{u} + (\boldsymbol{I} - \boldsymbol{B}\boldsymbol{B}_\theta^{-1})\boldsymbol{\tau}, \quad (4)$$

and of an impedance control loop, which provides the desired Cartesian impedance behaviour:

$$\boldsymbol{u} = -\boldsymbol{J}(\boldsymbol{\theta})^T(\boldsymbol{K}_x\tilde{\boldsymbol{x}} + \boldsymbol{D}_x\dot{\boldsymbol{x}}(\boldsymbol{\theta})) + \bar{\boldsymbol{g}}(\boldsymbol{\theta}) \ , \quad (5)$$

$$\tilde{\boldsymbol{x}}(\boldsymbol{\theta}) = \boldsymbol{f}(\boldsymbol{\theta}) - \boldsymbol{x}_s \quad (6)$$

$\boldsymbol{u}$ is an intermediate control input, $\boldsymbol{K}_x$ and $\boldsymbol{D}_x$ are the p.d. matrices of desired stiffness and damping. $\boldsymbol{x}_s$ is the desired tip position and $\boldsymbol{x}(\boldsymbol{\theta}) = \boldsymbol{f}(\boldsymbol{\theta})$ is the tip position computed based on the motor position measurements. $\boldsymbol{J}(\boldsymbol{\theta}) = \frac{\partial \boldsymbol{f}(\boldsymbol{\theta})}{\boldsymbol{\theta}}$ is the manipulator Jacobian. The gravity compensation term $\bar{\boldsymbol{g}}(\boldsymbol{\theta})$ is a function of the motor position and is designed in such a way that it provides exact gravity compensation in static case. The resulting close loop system is given by:

$$\boldsymbol{M}(\boldsymbol{q})\ddot{\boldsymbol{q}} + \boldsymbol{C}(\boldsymbol{q},\dot{\boldsymbol{q}})\dot{\boldsymbol{q}} + \boldsymbol{g}(\boldsymbol{q}) = \boldsymbol{\tau} + \boldsymbol{\tau}_{ext} \quad (7)$$

$$\boldsymbol{B}_\theta\ddot{\boldsymbol{\theta}} + \boldsymbol{J}(\boldsymbol{\theta})^T(\boldsymbol{K}_x\tilde{\boldsymbol{x}}(\boldsymbol{\theta}) + \boldsymbol{D}_x\dot{\boldsymbol{x}}(\boldsymbol{\theta})) + \boldsymbol{\tau} = \bar{\boldsymbol{g}}(\boldsymbol{\theta}) \quad (8)$$

Very important for the passivity of the impedance subsystem is the usage of functions depending on motor position $\boldsymbol{\theta}$ both for the gravity compensation $\bar{\boldsymbol{g}}(\boldsymbol{\theta})$, as well as for the forward kinematics model $\boldsymbol{x}(\boldsymbol{\theta}) = \boldsymbol{f}(\boldsymbol{\theta})$. Under these conditions, the asymptotic stability was proven in [7] for the regulation case.

In order to achieve high control performance with an implementation of this control concept on a real robot, some extensions of the basic structure are necessary. They regard the injection of damping into the torque loop in order to enhance robustness, as well as the design of the Cartesian stiffness and damping matrices. Since the impedance is implemented using the forward kinematics based on the motor position, the desired stiffness matrix needs to be appropriately designed in order to take into account also effects of the joint stiffness on the resulting link side Cartesian stiffness. Also, since the natural (variable) Cartesian inertia of the manipulator is not modi£ed by the controller, an appropriate variable damping matrix has to be designed in order achieve a well damped behaviour of the system.

In [7] we focused on the presentation of the main ideas and tried therefore to keep the complexity of the equations moderate. In this paper, various extensions will be presented by repeatedly referring to the basic control structure and the associated stability proof and by pointing out the speci£c differences.

For performance validation of the new controller, two experiments are presented in the £nal part of the paper. The effectiveness of the controller has been validated also during the past two years in several applications regarding teaching by demonstration (£g. 1) in service robotics scenarios.

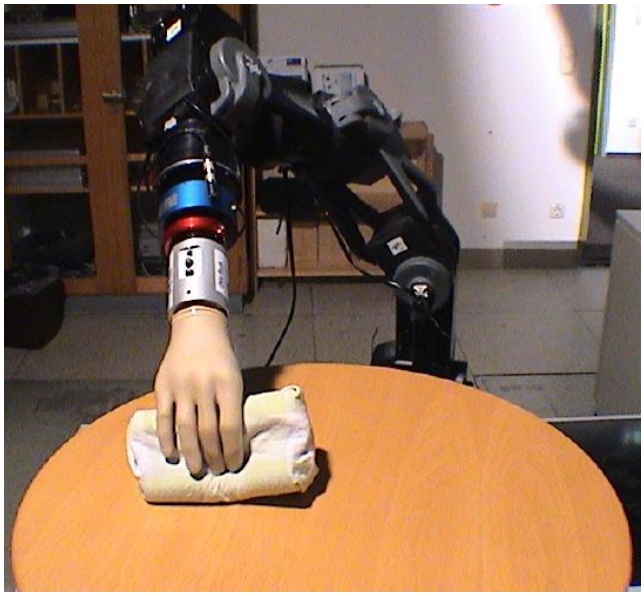

Fig. 1. DLR light-weight robot, generation II, using impedance control in a table wiping application.

II. Implementation of a full state feedback controller

The equivalent version of (5) in joint coordinates is:

$$\boldsymbol{u} = -\boldsymbol{K}_\theta(\boldsymbol{\theta} - \boldsymbol{\theta}_s) - \boldsymbol{D}_\theta\dot{\boldsymbol{\theta}} + \bar{\boldsymbol{g}}(\boldsymbol{\theta}) \tag{9}$$

This controller structure together with (4) can be rewritten as:

$$\boldsymbol{\tau}_m = -\boldsymbol{K}_P\tilde{\boldsymbol{\theta}} - \boldsymbol{K}_D\dot{\boldsymbol{\theta}} + \boldsymbol{K}_T(\bar{\boldsymbol{g}}(\boldsymbol{\theta}) - \boldsymbol{\tau}) + \bar{\boldsymbol{g}}(\boldsymbol{\theta}) \tag{10}$$

Herefore, the notations $\boldsymbol{K}_P = \boldsymbol{B}\boldsymbol{B}_\theta^{-1}\boldsymbol{K}_\theta$, $\boldsymbol{K}_D = \boldsymbol{B}\boldsymbol{B}_\theta^{-1}\boldsymbol{D}_\theta$, $\boldsymbol{K}_T = \boldsymbol{B}\boldsymbol{B}_\theta^{-1} - \boldsymbol{I}$ were used. $\tilde{\boldsymbol{\theta}} = \boldsymbol{\theta} - \boldsymbol{\theta}_s$ is the error between measured and desired motor position. Looked this way, the controller structure consists of a partial state feedback with constant gains. A complete state vector is given by, e.g., $\{\dot{\boldsymbol{\theta}}, \boldsymbol{\theta}, \dot{\boldsymbol{\tau}}, \boldsymbol{\tau}\}$[1]. Consequently, there is a direct relationship between (10) and the state feedback controller with constant gains and gravity compensation proposed in [1], [2], where the following controller was introduced for position and impedance control on joint level:

$$\begin{aligned}\boldsymbol{\tau}_m &= -\boldsymbol{K}_P\tilde{\boldsymbol{\theta}} - \boldsymbol{K}_D\dot{\boldsymbol{\theta}} \\ &\quad + \boldsymbol{K}_T(\boldsymbol{g}(\boldsymbol{q}_0) - \boldsymbol{\tau}) - \boldsymbol{K}_s\dot{\boldsymbol{\tau}} + \boldsymbol{g}(\boldsymbol{q}_0)\end{aligned} \tag{11}$$

The major structural differences between the two controllers consist in the way of compensating the gravity term and in the additional feedback of the torque derivative $\dot{\boldsymbol{\tau}}$ in (11). The replacement of $\boldsymbol{g}(\boldsymbol{q}_0)$ with $\bar{\boldsymbol{g}}(\boldsymbol{\theta})$) provides asymptotic stability for any p.d. position feedback gain matrix $\boldsymbol{K}_P$. This is important, especially for the implementation of impedance control with low desired stiffness. The extension of (4, 5) to a full state feedback by adding the torque derivative feedback will be addressed in detail in section II-A.

Besides of these structural differences, the design idea presented in this work provides a physical, passivity based interpretation of the torque feedback and a simple and intuitive way of implementing an impedance behaviour on joint level. In [2], the design idea for obtaining the constant gains for the impedance controller, was to do a linear pole placement design for the worst case con£guration (regarding e.g., the diagonal terms of the mass matrix $\boldsymbol{M}(\boldsymbol{q})$, independently for each joint. As an additional constraint, the gains have to lead to the desired link side stiffness (see sec. III), and the desired damping. In contrast, the new approach focuses on an intuitive and transparent way of designing the impedance, which can be easily extended to the Cartesian case. The dynamics of the closed loop (i.e., the poles in the linear, 1dof[2] case) are resulting in an implicit way. The closed loop dynamics approximates the desired impedance behaviour increasingly accurate, the lower $\boldsymbol{B}_\theta$ can be chosen. Notice that even with a full state feedback, it is not possible to independently choose both the desired link side stiffness (as a reaction on external disturbances $\boldsymbol{\tau}_{ext}$) and the desired dynamics of impedance controller (as a response on position steps). This would require the additional measurement of the external torque $\boldsymbol{\tau}_{ext}$ or, alternatively, of the link acceleration $\ddot{\boldsymbol{q}}$.

Based on the mentioned analogy of the two controllers, the extension of the new impedance controller to a full state feedback will be introduced next.

A. Considering a robot model with joint damping in parallel to the elasticity

The controller (11) was designed for a robot model, which contained in (1), (2) an additional diagonal p.d. damping matrix $\boldsymbol{D}$ in parallel to the joint elasticity:

$$\begin{aligned}\boldsymbol{M}(\boldsymbol{q})\ddot{\boldsymbol{q}} + \boldsymbol{C}(\boldsymbol{q},\dot{\boldsymbol{q}})\dot{\boldsymbol{q}} + \boldsymbol{g}(\boldsymbol{q}) &= \boldsymbol{\tau} + \boldsymbol{D}\boldsymbol{K}^{-1}\dot{\boldsymbol{\tau}} + \boldsymbol{\tau}_{ext} \\ \boldsymbol{B}\ddot{\boldsymbol{\theta}} + \boldsymbol{\tau} + \boldsymbol{D}\boldsymbol{K}^{-1}\dot{\boldsymbol{\tau}} &= \boldsymbol{\tau}_m\end{aligned} \tag{12}$$

This damping term, which is in many cases practically relevant, is mostly ignored in literature, in order to obtain a system which is static state feedback linearizable [4], [3]. The analysis of the system in this work relies on passivity properties, similar to [1], and therefore the addition of joint damping is rather bene£cial for the stability and performance properties, as it will turn out in the next section.

B. Adding a simple feedback of the torque derivative

Consider the following extension of the torque controller (4) by adding the feedback of the torque derivative:

$$\boldsymbol{\tau}_m = \boldsymbol{B}\boldsymbol{B}_\theta^{-1}\boldsymbol{u} + (\boldsymbol{I} - \boldsymbol{B}\boldsymbol{B}_\theta^{-1})(\boldsymbol{\tau} + \boldsymbol{D}\boldsymbol{K}^{-1}\dot{\boldsymbol{\tau}}), \tag{13}$$

The equations of the controlled system become:

$$\begin{aligned}&\boldsymbol{M}(\boldsymbol{q})\ddot{\boldsymbol{q}} + \boldsymbol{C}(\boldsymbol{q},\dot{\boldsymbol{q}})\dot{\boldsymbol{q}} + \boldsymbol{g}(\boldsymbol{q}) = \boldsymbol{\tau} + \boldsymbol{D}\boldsymbol{K}^{-1}\dot{\boldsymbol{\tau}} + \boldsymbol{\tau}_{ext} \\ &\boldsymbol{B}_\theta\ddot{\boldsymbol{\theta}} + \boldsymbol{J}(\boldsymbol{\theta})^T(\boldsymbol{K}_x\tilde{\boldsymbol{x}}(\boldsymbol{\theta}) + \boldsymbol{D}_x\dot{\boldsymbol{x}}(\boldsymbol{\theta})) + \boldsymbol{\tau} + \boldsymbol{D}\boldsymbol{K}^{-1}\dot{\boldsymbol{\tau}} = \boldsymbol{0}\end{aligned} \tag{14}$$

[1]Alternatively, if a joint torque sensor is not available, the state vector $\{\dot{\boldsymbol{\theta}}, \boldsymbol{\theta}, \dot{\boldsymbol{q}}, \boldsymbol{q}\}$ can be used, as mostly done in the literature. The two state vectors are, of course, linearly related through (3). Nevertheless, using a torque sensor turned out to be in practice considerably more robust to unmodeled dynamics.

[2]dof - degrees of freedom

With the notation $\boldsymbol{\tau}_a = \boldsymbol{\tau} + \boldsymbol{D}\boldsymbol{K}^{-1}\dot{\boldsymbol{\tau}}$ it is clear, following [7], that the two subsystems in (14) are passive with respect to the variables $\{\boldsymbol{\tau}_a, \dot{\boldsymbol{q}}\}$. The same Lyapunov function as in [7] can be used for the analysis:

$$\begin{aligned} V &= \frac{1}{2}\Big[\dot{\boldsymbol{q}}^T\boldsymbol{M}(\boldsymbol{q})\dot{\boldsymbol{q}} + \dot{\boldsymbol{\theta}}^T\boldsymbol{B}_\theta\dot{\boldsymbol{\theta}} + (\boldsymbol{\theta}-\boldsymbol{q})^T\boldsymbol{K}(\boldsymbol{\theta}-\boldsymbol{q}) \\ &\quad + \tilde{\boldsymbol{x}}(\boldsymbol{\theta})^T\boldsymbol{K}_x\tilde{\boldsymbol{x}}(\boldsymbol{\theta})\Big] - V_{\bar{g}}(\boldsymbol{\theta}) + V_g(\boldsymbol{q}), \end{aligned} \tag{15}$$

where $V_{\bar{g}}(\boldsymbol{\theta})$ and $V_g(\boldsymbol{q})$ are the potential functions for $\bar{\boldsymbol{g}}(\boldsymbol{\theta}))$ and $\boldsymbol{g}(\boldsymbol{q})$ respectively. However, the derivative $\dot{V}$ changes to:

$$\dot{V}(\boldsymbol{q}, \dot{\boldsymbol{q}}, \boldsymbol{\theta}, \dot{\boldsymbol{\theta}}) = -\dot{\boldsymbol{x}}^T\boldsymbol{D}_x\dot{\boldsymbol{x}} - (\dot{\boldsymbol{\theta}} - \dot{\boldsymbol{q}})^T\boldsymbol{D}(\dot{\boldsymbol{\theta}} - \dot{\boldsymbol{q}}) \tag{16}$$

and is therefore also negative semide£nite. Consequently, the asymptotic stability properties proven in [7] are valid also in this case.

C. Full state feedback: general case

The asymptotic stability can be proven also for the case that (13) is replaced by a more general version of the torque controller:

$$\begin{aligned} \boldsymbol{\tau}_m &= \boldsymbol{B}\boldsymbol{B}_\theta^{-1}\boldsymbol{u} + \boldsymbol{\tau} + \boldsymbol{D}\boldsymbol{K}^{-1}\dot{\boldsymbol{\tau}} \\ &\quad - \boldsymbol{B}\boldsymbol{B}_\theta^{-1}(\boldsymbol{\tau} + \boldsymbol{K}_s\boldsymbol{K}^{-1}\dot{\boldsymbol{\tau}}) \end{aligned} \tag{17}$$

where $\boldsymbol{K}_s$ is an independent diagonal gain matrix for the torque derivative feedback, which satis£es the following condition:

$$\boldsymbol{D} > \frac{1}{4}(\boldsymbol{K}_s - \boldsymbol{D})^T(\boldsymbol{J}(\boldsymbol{\theta})^T\boldsymbol{D}_x\boldsymbol{J}(\boldsymbol{\theta}))^{-1}(\boldsymbol{K}_s - \boldsymbol{D}). \tag{18}$$

A sketch of the proof is given in the following. With the new control law (17), the second subsystem in (14) becomes

$$\boldsymbol{B}_\theta\ddot{\boldsymbol{\theta}} + \boldsymbol{J}(\boldsymbol{\theta})^T(\boldsymbol{K}_x\tilde{\boldsymbol{x}}(\boldsymbol{\theta}) + \boldsymbol{D}_x\dot{\boldsymbol{x}}(\boldsymbol{\theta})) + \boldsymbol{\tau} + \boldsymbol{K}_s\boldsymbol{K}^{-1}\dot{\boldsymbol{\tau}} = \boldsymbol{0} \tag{19}$$

Since the £rst subsystem in (14) remains unchanged, it is clear that the stability of the system depends on the passivity of (19). Consider the same storage function as in [7]:

$$\begin{aligned} S_\theta &= \frac{1}{2}\dot{\boldsymbol{\theta}}^T\boldsymbol{B}_\theta\dot{\boldsymbol{\theta}} + \frac{1}{2}(\boldsymbol{\theta}-\boldsymbol{q})^T\boldsymbol{K}(\boldsymbol{\theta}-\boldsymbol{q}) \\ &\quad + \frac{1}{2}\tilde{\boldsymbol{x}}(\boldsymbol{\theta})^T\boldsymbol{K}_x\tilde{\boldsymbol{x}}(\boldsymbol{\theta}) - V_{\bar{g}}(\boldsymbol{\theta}), \end{aligned} \tag{20}$$

which has been proven to be p.d.. Its time derivative is now:

$$\begin{aligned} \dot{S}_\theta &= -\dot{\boldsymbol{\theta}}^T\boldsymbol{J}(\boldsymbol{\theta})^T\boldsymbol{D}_x\boldsymbol{J}(\boldsymbol{\theta})\dot{\boldsymbol{\theta}} - (\dot{\boldsymbol{\theta}} - \dot{\boldsymbol{q}})^T\boldsymbol{D}(\dot{\boldsymbol{\theta}} - \dot{\boldsymbol{q}}) \\ &\quad + \dot{\boldsymbol{\theta}}^T(\boldsymbol{D} - \boldsymbol{K}_s)(\dot{\boldsymbol{\theta}} - \dot{\boldsymbol{q}}). \end{aligned} \tag{21}$$

This function is negative de£nite if condition (18) is ful£lled. This implies the passivity of (19). The asymptotic stability is then proven using the same Lyapunov function V as before, which is simply the sum of the storage functions of the two subsystems.

Remarks:

- The proposed controller can be regarded as a cascaded structure, with an inner torque control loop and an outer position control loop. However, in this case it is not necessary to use the somewhat restrictive singular perturbation argumentation for proving stability. Asymptotic stability can be proven for arbitrary joint stiffness and do not require a slower dynamics of the outer loop.
- The possibility of specifying the gains for a full state feedback extends the degrees of freedom in the design and enhances the system performance. The gain $\boldsymbol{K}_s$ in particular adds damping to the torque controller, increasing its robustness. As it will be discussed in sec. IV, the damping matrices can be then changed online to increase performance.

III. Specification of a link side stiffness

For the design of the impedance (9), (5), the desired stiffness was de£ned so far as a relation between the external torque and a position vector ($\boldsymbol{\theta}$ or $\boldsymbol{x}(\boldsymbol{\theta})$) based on motor side measurements: $\boldsymbol{K}_\theta = \frac{\partial \boldsymbol{\tau}_{ext}}{\partial \boldsymbol{\theta}}\big|_\Phi$ or $\boldsymbol{K}_x = \frac{\partial \boldsymbol{f}_{ext}}{\partial \boldsymbol{x}(\boldsymbol{\theta})}\Big|_\Phi$, where $\boldsymbol{F}_{ext}$ represents the external Cartesian force. The condition Φ represents the steady state, i.e. $\Phi \equiv \{\dot{\boldsymbol{\theta}} = 0,\, \ddot{\boldsymbol{\theta}} = 0,\, \dot{\boldsymbol{q}} = 0,\, \ddot{\boldsymbol{q}} = 0\}$. In this section, a speci£cation of a link side stiffness matrix, which takes into account the effects of joint elasticity, will be addressed.

A. The joint space version

Eq. (9) speci£es a relationship between the motor position and the external torque. In general, one would like to specify a stiffness of the form $\boldsymbol{K}_e = \frac{\partial \boldsymbol{\tau}_{ext}}{\partial \boldsymbol{q}}\Big|_\Phi$. From the closed loop equation of the joint version of the controller:

$$\boldsymbol{M}(\boldsymbol{q})\ddot{\boldsymbol{q}} + \boldsymbol{C}(\boldsymbol{q}, \dot{\boldsymbol{q}})\dot{\boldsymbol{q}} + \boldsymbol{g}(\boldsymbol{q}) = \boldsymbol{\tau} + \boldsymbol{\tau}_{ext} \tag{22}$$

$$\boldsymbol{B}_\theta\ddot{\boldsymbol{\theta}} + \boldsymbol{D}_\theta\dot{\boldsymbol{\theta}} + \boldsymbol{K}_\theta(\boldsymbol{\theta} - \boldsymbol{\theta}_s) + \boldsymbol{\tau} = \boldsymbol{0}, \tag{23}$$

it results that

$$\boldsymbol{K}_e = (\boldsymbol{K}_\theta^{-1} + \boldsymbol{K}^{-1})^{-1}. \tag{24}$$

For high values of $\boldsymbol{K}_\theta$ the resulting error may be quite large (up to 30% for the DLR robots). Consequently, given a p.d. matrix $\boldsymbol{K}_e$, with $(\boldsymbol{K} - \boldsymbol{K}_e)$ also p.d., one should compute the required matrix $\boldsymbol{K}_\theta$ from (24) as:

$$\boldsymbol{K}_\theta = (\boldsymbol{K}_e^{-1} - \boldsymbol{K}^{-1})^{-1}. \tag{25}$$

B. Cartesian space version

While for the speci£cation of the joint stiffness an exact solution has been found, only an approximation can be done in the Cartesian case.

The link side Cartesian stiffness is $\boldsymbol{K}_{e,x} = \frac{\partial \boldsymbol{F}_{ext}}{\partial \boldsymbol{x}(\boldsymbol{q})}\Big|_\Phi$. Around the desired position $\boldsymbol{x}_s$, i.e. for small displacements $\tilde{\boldsymbol{x}}$, $\boldsymbol{K}_{e,x}$ can be then approximated (with $\boldsymbol{J}(\boldsymbol{q}) \approx \boldsymbol{J}(\boldsymbol{\theta}) \approx \boldsymbol{J}(\boldsymbol{q}_0) \approx \boldsymbol{J}(\boldsymbol{\theta}_0)$) as:

$$\boldsymbol{K}_{e,x} = [\boldsymbol{K}_x^{-1} + \boldsymbol{J}(\boldsymbol{\theta}_0)\boldsymbol{K}^{-1}\boldsymbol{J}(\boldsymbol{\theta}_0)^T]^{-1}. \tag{26}$$

It is then possible to compute the required matrix $\boldsymbol{K}_x$ around the equilibrium position:

$$\boldsymbol{K}_x = [\boldsymbol{K}_{e,x}^{-1} - \boldsymbol{J}(\boldsymbol{\theta}_0)\boldsymbol{K}^{-1}\boldsymbol{J}(\boldsymbol{\theta}_0)^T]^{-1}. \tag{27}$$

Of course, one has to make sure that $\boldsymbol{K}_x$ remains positive de£nite.

IV. Damping Design

In sec. II-A it was mentioned that it is possible to use variable damping matrices $\boldsymbol{D}_x$ and $\boldsymbol{K}_s$. This becomes obvious, when looking at the Lyapunov function V and its time derivative $\dot{V}$ along the system trajectories: V does not contain neither $\boldsymbol{D}_x$ nor $\boldsymbol{K}_s$. Both matrices appear only in $\dot{V}$, what is not surprising, since they are responsible for the energy dissipation in the system. It is therefore possible to use any kind of variable, p.d. damping matrix $\boldsymbol{D}_x$ and any matrix $\boldsymbol{K}_s$ satisfying (18), while preserving the stability properties. In particular, those matrices can be designed based on gain scheduling as $\boldsymbol{D}_x(\boldsymbol{\theta})$ and $\boldsymbol{K}_s(\boldsymbol{\theta})$, using the motor position $\boldsymbol{\theta}$ as a scheduling variable. The motivation and two possible approaches to do this will be next presented for the matrix $\boldsymbol{D}_x$.

Consider the equations of the closed loop dynamics (7, 8),

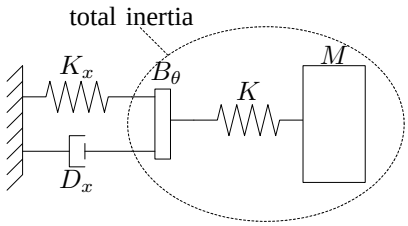

Fig. 2. Approximations for the damping design.

under the typical singular perturbation assumption for the reduced model, namely $\boldsymbol{K} \to \infty$. This implies $\boldsymbol{q} \approx \boldsymbol{\theta}$ (see also £g.2). For simplicity, assume further that the mass matrix $\boldsymbol{M}(\boldsymbol{q})$ is varying slowly, so that its derivative can also be neglected[3]. Then the following closed loop dynamics approximation can be used for the design:

$$(\boldsymbol{M}(\boldsymbol{\theta}) + \boldsymbol{B}_\theta)\ddot{\boldsymbol{\theta}} + \boldsymbol{J}(\boldsymbol{\theta})^T(\boldsymbol{K}_x\tilde{\boldsymbol{x}}(\boldsymbol{\theta}) + \boldsymbol{D}_x\dot{\boldsymbol{x}}(\boldsymbol{\theta})) = \boldsymbol{0} \qquad (28)$$

or

$$\boldsymbol{\Lambda}(\boldsymbol{\theta})\ddot{\tilde{\boldsymbol{x}}}(\boldsymbol{\theta}) + \boldsymbol{D}_x\dot{\tilde{\boldsymbol{x}}}(\boldsymbol{\theta}) + \boldsymbol{K}_x\tilde{\boldsymbol{x}}(\boldsymbol{\theta}) = \boldsymbol{0} \qquad (29)$$

by using the notation $\boldsymbol{\Lambda}(\boldsymbol{\theta}) = (\boldsymbol{J}(\boldsymbol{\theta})(\boldsymbol{M}(\boldsymbol{\theta}) + \boldsymbol{B}_\theta)^{-1}\boldsymbol{J}(\boldsymbol{\theta})^T)^{-1}$ for a Cartesian mass matrix. The question comes up, how to design the desired damping matrix $\boldsymbol{D}_x$ depending on the desired stiffness and the actual value of $\boldsymbol{\Lambda}(\boldsymbol{\theta})$. What the user may wish to specify for an application, is a well de£ned damping behaviour in every Cartesian direction (e.g. a critically damped one). It is then obvious that the damping matrix $\boldsymbol{D}_x$ cannot be constant, but has to be chosen as a function of $\boldsymbol{\Lambda}(\boldsymbol{\theta})$. Choosing a variable damping matrix rather than a constant one leads to signi£cant performance improvements in practice, even using the mentioned approximations for the design.

[3]Notice again that all these simpli£cations are done only for the purpose of damping design and do not affect in any sense the stability of the system, but can in¤uence merely the performance parameters.

A. Factorization Design

If the eigenvalues of the impedance dynamics should be all real, it can be easily seen that this can be achieved by a damping matrix of the form $\boldsymbol{D}_x = \boldsymbol{A}\boldsymbol{K}_{x1} + \boldsymbol{K}_{x1}\boldsymbol{A}$, where $\boldsymbol{A}$ and $\boldsymbol{K}_{x1}$ are de£ned as $\boldsymbol{A}\boldsymbol{A} = \boldsymbol{\Lambda}$ and $\boldsymbol{K}_{x1}\boldsymbol{K}_{x1} = \boldsymbol{K}_x$ respectively. (29) can then be factorized as

$$\boldsymbol{A}\big(\boldsymbol{A}\ddot{\tilde{\boldsymbol{x}}}(\boldsymbol{\theta}) + \boldsymbol{K}_{x1}\dot{\tilde{\boldsymbol{x}}}(\boldsymbol{\theta})\big) + \qquad (30)$$

$$+\boldsymbol{K}_{x1}\big(\boldsymbol{A}\dot{\tilde{\boldsymbol{x}}}(\boldsymbol{\theta}) + \boldsymbol{K}_{x1}\tilde{\boldsymbol{x}}(\boldsymbol{\theta})\big) = \boldsymbol{0}\,. \qquad (31)$$

With the substitution $\boldsymbol{A}\dot{\tilde{\boldsymbol{x}}}(\boldsymbol{\theta}) + \boldsymbol{K}_{x1}\tilde{\boldsymbol{x}}(\boldsymbol{\theta}) = \boldsymbol{w}$, this leads to the system

$$\boldsymbol{A}\dot{\tilde{\boldsymbol{x}}}(\boldsymbol{\theta}) + \boldsymbol{K}_{x1}\tilde{\boldsymbol{x}}(\boldsymbol{\theta}) = \boldsymbol{w} \qquad (32)$$

$$\boldsymbol{A}\dot{\boldsymbol{w}} + \boldsymbol{K}_{x1}\boldsymbol{w} = \boldsymbol{0}\,, \qquad (33)$$

which has n pairs of equal, real eigenvalues as desired. A heuristic design approach may then be to choose a general damping design of the form

$$\boldsymbol{D}_x = \boldsymbol{A}\boldsymbol{D}_\xi\boldsymbol{K}_{x1} + \boldsymbol{K}_{x1}\boldsymbol{D}_\xi\boldsymbol{A}\,, \qquad (34)$$

where $\boldsymbol{D}_\xi = \mathrm{diag}\{\xi_i\}$ is a diagonal matrix and $0 \le \xi_i \le 1$ (0 for undamped behaviour and 1 for real eigenvalues). For a wide stiffness range this approach leads indeed to numerical eigenvalues with a damping very close to the desired one.

B. Double Diagonalization Design

Another, maybe more elegant approach to the design of the damping matrix can be developed based on the generalized eigenvalue problem known from matrix algebra [5]:
Given a symmetric positive de£nite $n \times n$ matrix $\boldsymbol{\Lambda}$ and a symmetric $n \times n$ matrix $\boldsymbol{K}_x$, a $n \times n$ nonsingular matrix $\boldsymbol{Q}$ can be found, such that $\boldsymbol{\Lambda} = \boldsymbol{Q}\boldsymbol{Q}^T$ and $\boldsymbol{K}_x = \boldsymbol{Q}\boldsymbol{K}_{x0}\boldsymbol{Q}^T$ for some diagonal matrix $\boldsymbol{K}_{x0}$.
By choosing the damping matrix as:

$$\boldsymbol{D}_x = 2\boldsymbol{Q}\boldsymbol{D}_\xi\boldsymbol{K}_{x0}^{1/2}\boldsymbol{Q}^T\,, \qquad (35)$$

an error dynamics of the form

$$\boldsymbol{Q}\boldsymbol{Q}^T\ddot{\tilde{\boldsymbol{x}}}(\boldsymbol{\theta}) + 2\boldsymbol{Q}\boldsymbol{D}_{\xi d}\boldsymbol{K}_{x0}^{1/2}\boldsymbol{Q}^T\dot{\tilde{\boldsymbol{x}}}(\boldsymbol{\theta}) + \qquad (36)$$

$$\boldsymbol{Q}\boldsymbol{K}_{x0}\boldsymbol{Q}^T\tilde{\boldsymbol{x}}(\boldsymbol{\theta}) = \boldsymbol{0}$$

can be obtained. This leads in the new coordinates $\boldsymbol{w} = \boldsymbol{Q}^T\tilde{\boldsymbol{x}}(\boldsymbol{\theta})$ to a system of n decoupled equations with the requested damping behaviour:

$$\ddot{\boldsymbol{w}} + 2\boldsymbol{D}_\xi\boldsymbol{K}_{x0}^{1/2}\dot{\boldsymbol{w}} + \boldsymbol{K}_{x0}\boldsymbol{w} = \boldsymbol{0}\,. \qquad (37)$$

As mentioned before, $\boldsymbol{M}$ and thus also $\boldsymbol{Q}$ is here assumed to be quasi-static. Notice that the decoupling can be achieved only in some particular directions, which are given by $\boldsymbol{Q}$ and hence depend on $\boldsymbol{\Lambda}$ and $\boldsymbol{K}_x$. This is not surprising, since the controller does not provide a decoupling of the mass matrix. Consequently, if the system is excited, oscillations will occur decoupled and with the desired damping behaviour only in those special directions.

V. EXPERIMENTS

Two experiments for the validation of the proposed controller structure will be presented in this section. The experiments are related to two typical application areas for impedance control: the stable and safe interaction of the robot with humans and the contact with unknown, stiff but passive environments. The controller version (5),(17) is used during the experiments. Notice that the estimation of $\dot{\boldsymbol{\tau}}$ through differentiation of the joint torque measurement is practically feasible for ¤exible joint robots, since $\boldsymbol{\tau}$ as well as $\dot{\boldsymbol{\tau}}$ are state variables (and as such they are smooth signals). In the case of the DLR light-weight robots, which have torque sensors placed after the gearbox in each joint, only a £rst order low pass £ltering at 300Hz is used after the differentiation.

A. Interaction with a human user

The £rst experiment tests the accuracy of the controlled Cartesian impedance during the interaction with a human user. The commanded values of the stiffness $\boldsymbol{K}_x$ are summarized in table I. The robot is commanded to display a signi£cantly more compliant behaviour in the x-direction then in the y-direction. The values of the damping in each direction are chosen such that the system is critically damped, with the damping design method from section IV-B. The user grasps the robot at the end-effector during the experiment and exerts forces (mainly) in the $x-y$ plane. The forces are measured at the tip of the arm using a 6dof force-torque sensor. [4] Fig. 4 displays the

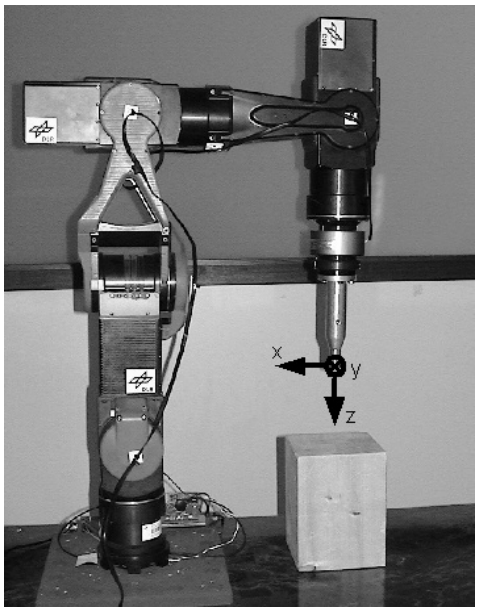

Fig. 3. The experimental setup with the DLR-light-weight-robot II for experiment V-B.

measured forces. Fig. 5 contains the corresponding position plots. The force-position plots for the x- and y-directions, together with the desired static dependency are shown in £g. 6 and 7 respectively. The mean slope of the measurements £ts very well with the desired slope. The "hysteresis-like" shape of the measurements is due to the damping of the system and corresponds to the commanded critical damping. In order to prove this, a simulation result is also plotted in the same £gure. The force-torque measurement is the input to a simulation of the ideal (desired) impedance with the position vector as an output.[5] The measurements are quite similar to the simulation, both for low and high stiffness, despite of the sensitivity of such an integration method with respect to force offsets.

TABLE I

DESIRED VALUES FOR THE DIAGONAL CARTESIAN STIFFNESS MATRIX FOR EXPERIMENT V-A

x	y	z	roll [6]	pitch	yaw
800 $\frac{\mathrm{N}}{\mathrm{m}}$	5000 $\frac{\mathrm{N}}{\mathrm{m}}$	5000 $\frac{\mathrm{N}}{\mathrm{m}}$	300 $\frac{\mathrm{Nm}}{\mathrm{rad}}$	300 $\frac{\mathrm{Nm}}{\mathrm{rad}}$	300 $\frac{\mathrm{Nm}}{\mathrm{rad}}$

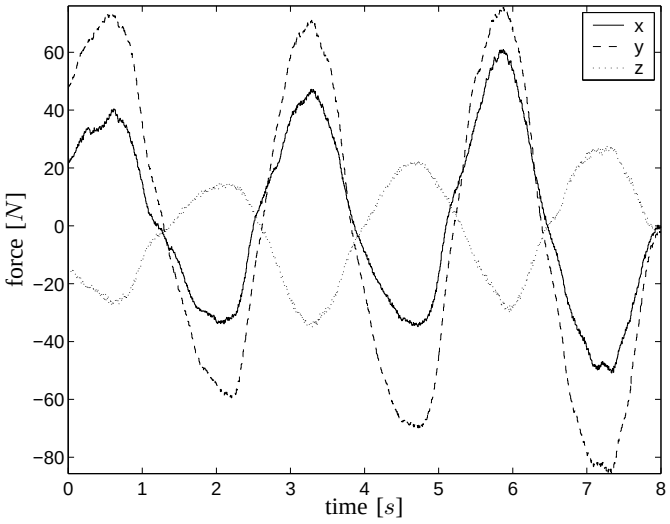

Fig. 4. Forces exerted on the robot by the user. (continuous line: force in x direction, dashed line: force in y direction, dotted line: force in z direction).

B. Impact on a stiff surface

The second experiment shows the ef£ciency of the impedance controller during the impact of the robot with a stiff surface. The manipulator is commanded to move in the vertical (z) direction. After the impact with a wooden surface, the force at the tip increases proportional to the position error. The commanded stiffness values for this experiment are summarized in table II. The stiffness in z-direction is low, in order to have a reasonable low steady state force. Also in this experiment, the commanded damping value is $\xi_x = 0.7$.

[4]The sensor measurements at the tip are used only for validation, they are not needed for the control.

[5]The simulation contains some simpli£cations and uncertainties: $\boldsymbol{M}(\boldsymbol{q})$ and $\boldsymbol{J}(\boldsymbol{q})$ are assumed to be constant during the movement. Also, only a simpli£ed friction model (for the uncompensated joint friction re¤ected to the tip) is considered.

[6]The values for the rotational stiffness were deliberately chosen high, so that the particular representation of orientations for the Cartesian position has no signi£cant effects on the results (see also [6], [9]).

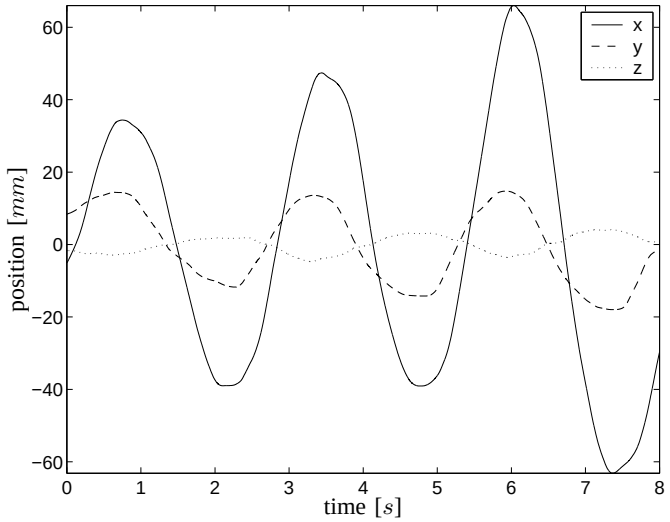

Fig. 5. Cartesian position displacement, computed based on the motor position. (continuous line: displacement in x direction, dashed line: displacement in y direction, dotted line: displacement in zv direction).

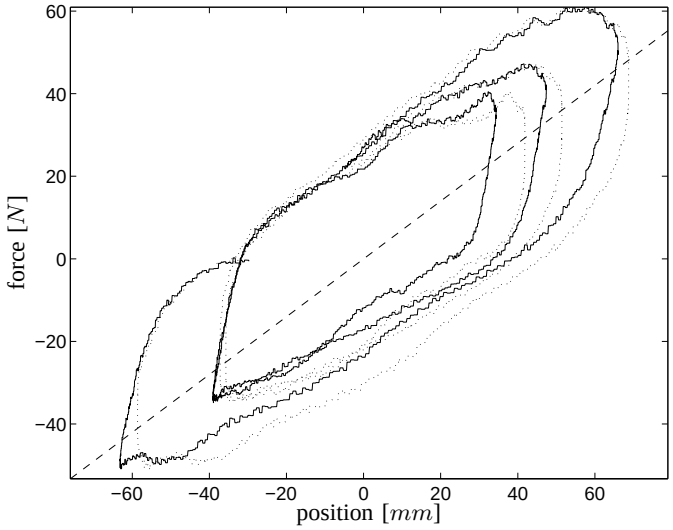

Fig. 6. Position and force in x-direction. The linear slope (dashed line) represents the desired stiffness. The dotted line is the result of the simulation.

The £gures 9 and 10 are displaying the position and the force in z-direction. Notice that the duration of the force peak generated during the dissipation of the kinetic energy is very short. (It is shorter than the $6\,\mathrm{ms}$ sampling rate used for the force-torque sensor). This is achieved on one side due the low mass of the manipulator. On the other side, the motor inertia is considerably reduced by the torque feedback. This leads to a reduction of the link side Cartesian mass in z direction by a factor of 3. Due to the passivity properties of the manipulator and to the high sampling rate of the torque control (see £g 8), no stability problems are encountered during the impact phase. Such problems are often present in case of force control of industrial robots using a force-torque sensor at the tip and require the reduction of the approaching velocity.

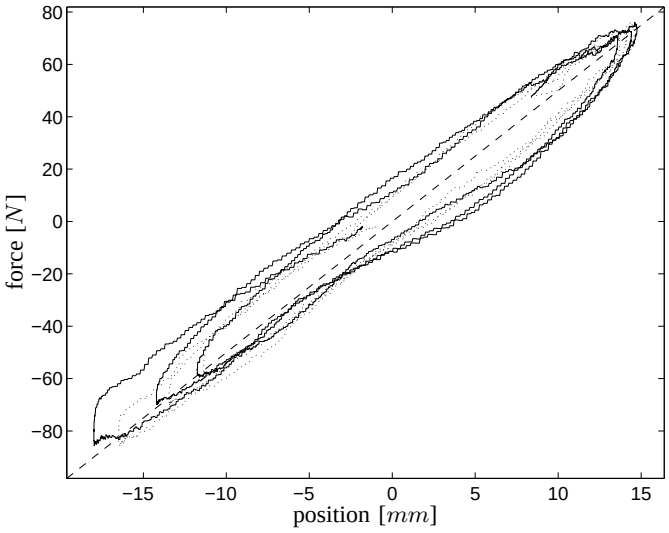

Fig. 7. Position and force in y-direction. The linear slope (dashed line) represents the desired stiffness. The dotted line is the result of the simulation.

TABLE II
DESIRED VALUES FOR THE DIAGONAL CARTESIAN STIFFNESS MATRIX FOR EXPERIMENT V-B

x	y	z	roll [7]	pitch	yaw
5000 $\frac{\mathrm{N}}{\mathrm{m}}$	5000 $\frac{\mathrm{N}}{\mathrm{m}}$	700 $\frac{\mathrm{N}}{\mathrm{m}}$	300 $\frac{\mathrm{Nm}}{\mathrm{rad}}$	300 $\frac{\mathrm{Nm}}{\mathrm{rad}}$	300 $\frac{\mathrm{Nm}}{\mathrm{rad}}$

VI. CONCLUSIONS

A new, physically motivated approach to Cartesian impedance control for ¤exible joint robots was presented in this work. The paper [7] introduced the main idea of reducing the apparent motor inertia by torque feedback and of implementing the gravity compensation and an impedance controller based on the motor position in a second step. A detailed passivity and stability analysis for the basic structure of the controller was given. The proof imposes no other restrictions to the stiffness and damping matrices than their positive de£niteness. It was shown that the closed loop system can be regarded as a feedback connection of passive blocks. As such it is robust against model uncertainties related to the rigid body dynamics, payload or contacted environment.
The second paper augments the controller structure in some practical aspects, in order to enhance robustness, performance and generality of the approach. The controller is extended to include the mostly avoided case of damped springs in the joints. The extension to full state feedback, including the torque derivative, provides an additional degree of freedom for the design. The design of variable damping matrices allow an accurate tuning of the desired impedance. A way of providing exact Cartesian stiffness (on link side) while using the mentioned motor position feedback was introduced. Finally, the controller performance was evaluated in two experiments, in which the robot interacted with a human user and with a stiff environment.

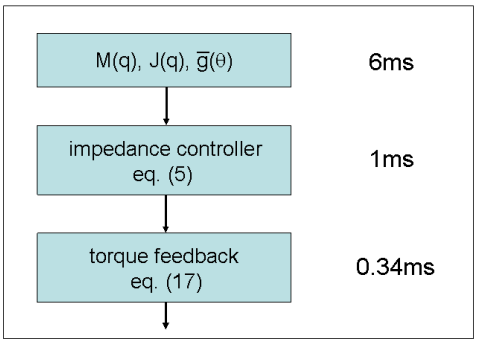

Fig. 8. Sampling rates for the implementation of the impedance controller on the DLR light-weight robots.

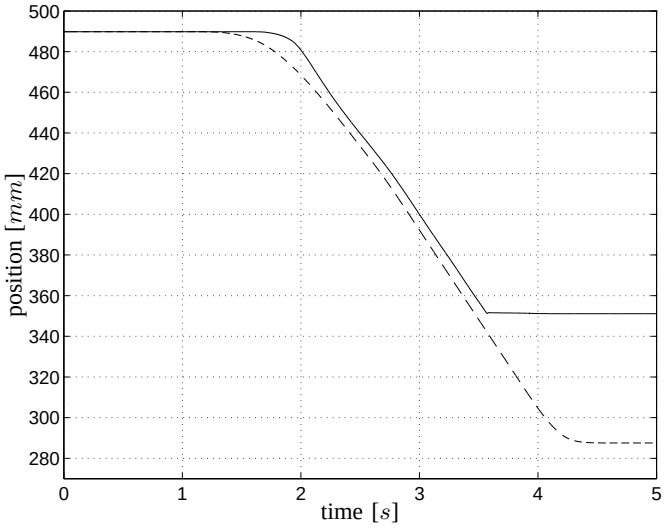

Fig. 9. Position in z direction for the impact experiment. (continuous line: measured position, dashed line: desired position).

It is remarkable that this controller was easy to implement even on a 7 dof robot and proved to work reliably in several applications already. The controller requires only the measurement of the position and torque as well as the estimation of their £rst derivatives. No estimation of higher order derivatives is required. This keeps the controller structure relatively simple and robust to model uncertainties, while providing a performant vibration damping due to complete state feedback.

REFERENCES

[1] A. Albu-Schäffer, G. Hirzinger, "A Globally Stable State-feedback Controller for Flexible Joint Robots", *Journal of Advanced Robotics, Special Issue: Selected Papers from IROS 2000, 2001, Vol. 15, Nr. 8, pp. 799-814*.

[2] A. Albu-Schäffer, "Regelung von Robotern mit elastischen Gelenken am Beispiel der DLR-Leichtbauarme", *Ph.D. thesis, Technische Universität München, April, 2002*.

[3] B. Brogliato and R. Ortega and R. Lozano "Global Tracking Controllers for Flexible-joint Manipulators: a Comparative Study" *Automatica, Vol. 31, No.7, pp941-956, 1995*

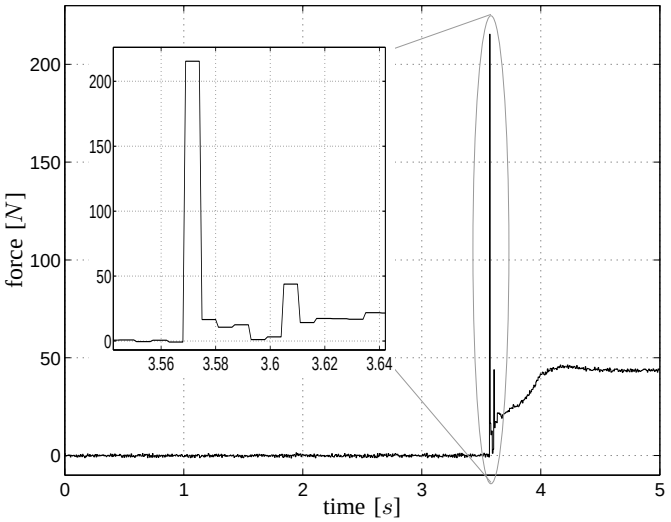

Fig. 10. Force in z direction for the impact experiment.

[4] A. De Luca and P. Lucibello "A General Algorithm for Dynamic Feedback Linearization of Robots with Elastic Joints" *ICRA, pp. 504-510 , 1998*.

[5] D. Harville "Matrix Algebra from a Statistician's Perspective". *Springer-Verlag, 1997*.

[6] C. Natale, "Interaction Control of Robot Manipulators: Six-Degrees-of-Freedom Tasks", *Springer Verlag, 2003*.

[7] C. Ott, A. Albu-Schäffer, A. Kugi, S. Stramigioli, G. Hirzinger, "A passivity based Cartesian Impedance Controller for ¤exible joint robots - Part I: Torque feedback and gravity compensation", *submitted to ICRA 2004*.

[8] M. Spong, "Modeling and Control of Elastic Joint Robots", *IEEE Journal of Robotics and Automation, 1987, Vol. 3, pp. 291-300*.

[9] S. Stramigioli and H. Bruyninckx, " Geometry and Screw Theory for Constrained and Unconstrained Robot ", *Tutorial at ICRA, 2001*

[10] P. Tomei, "A Simple PD Controller for Robots with Elastic Joints", *IEEE Transactions on Automatic Control, vol. 35, pp. 1208-1213, 1991*.